applied sciences

MDPI

Article

Accumulation and Emission of Water Vapor by Silica Gel Enriched with Carbon Nanotubes CNT-Potential Applications in Adsorption Cooling and Desalination Technology

Anna Pajdak [1,*], Anna Kulakowska [2], Jinfeng Liu [3], Katarzyna Berent [4], Mateusz Kudasik [1], Jaroslaw Krzywanski [2], Wojciech Kalawa [4], Karol Sztekler [4] and Norbert Skoczylas [1]

1 The Strata Mechanics Research Institute of the Polish Academy of Sciences, Reymonta 27, 30-059 Cracow, Poland; kudasik@imgpan.pl (M.K.); skoczylas@imgpan.pl (N.S.)
2 Faculty of Science and Technology, Jan Dlugosz University in Czestochowa, al. 13/15 Armii Krajowej, 42-200 Czestochowa, Poland; a.kulakowska@ujd.edu.pl (A.K.); j.krzywanski@ujd.edu.pl (J.K.)
3 School of Earth Sciences and Engineering, Sun Yat-sen University, Guangzhou 510275, China; liujinf5@mail.sysu.edu.cn
4 Faculty of Energy and Fuels, AGH University of Science and Technology, ul. A. Mickiewicza 30, 30-059 Cracow, Poland; kberent@agh.edu.pl (K.B.); kalawa@agh.edu.pl (W.K.); sztekler@agh.edu.pl (K.S.)
* Correspondence: pajdak@imgpan.pl

Abstract: This paper presents a study of the application of the properties of water vapor as a gas with high potential energy, strongly dependent on temperature and pressure. Analyses of water vapor sorption on two types of silica gels (SG) (90 wt.%) enriched with carbon nanotubes (CNTs) (10 wt.%), in the context of their application in the design of adsorption beds in adsorption cooling and desalination systems were conducted. The sorption experiments were performed by gravimetric method at a relative humidity of 0% < RH < 100% and temperatures of 298 K, 313 K, and 333 K. The addition of CNTs to SG caused a decrease in the sorption capacity and depended on the temperature. As the process temperature increased, a lower SG/CNT mixtures sorption capacity to vapor was obtained. The highest influence of CNTs was observed at the highest temperature, and the average decrease of sorption capacity was several percent. The ratio of SG/CNT sorption capacity to pure SG values was below 1 in most measurements.

Keywords: adsorption; sorption capacity; water vapor; silica gel; carbon nanotubes; CNT; pore structure

Citation: Pajdak, A.; Kulakowska, A.; Liu, J.; Berent, K.; Kudasik, M.; Krzywanski, J.; Kalawa, W.; Sztekler, K.; Skoczylas, N. Accumulation and Emission of Water Vapor by Silica Gel Enriched with Carbon Nanotubes CNT-Potential Applications in Adsorption Cooling and Desalination Technology. *Appl. Sci.* **2022**, *12*, 5644. https://doi.org/10.3390/app12115644

Academic Editor: Chang-Gu Lee

Received: 29 April 2022
Accepted: 30 May 2022
Published: 1 June 2022

1. Introduction

Greenhouse gases (GHGs) make up about 1% of all atmospheric gases. Many types of GHGs can trap heat in the atmosphere, the most active of which are carbon dioxide, methane, and nitrous oxide. Water vapor is the gas most significant in building the Earth's greenhouse effect. Its concentration alone in the atmosphere, however, does not cause climate change. However, water vapor is an amplifier of these changes because it is responsible for the strongest positive feedback in the climate system. The stronger the feedback, the more heat is trapped, and the feedback increases as other greenhouse gases increase.

Water vapor is the only greenhouse gas that is highly dependent on air temperature. The higher it is, the more of it there is in the atmosphere. For this reason, water vapor has been used for many years as an energy carrier in industrial and equipment production processes. It can contain five or six times more potential energy than water of the same mass. It allows energy storage, and the process is easy to control. For years, research has been conducted on a laboratory and industrial scale on the use of vapor for heat transfer. Reasons include the high heat transfer efficiency of steam with a relatively small heat transfer surface area.

Silica gel (SG) is an adsorbent often used in commercial applications such as adsorption cooling [1], drying [2–4], and desalination [5–7]. It has a low desorption temperature (<373 K) [8–10], which makes this material very suitable for use in adsorption chillers to utilize waste heat. Water vapor adsorption on silica gel is a physical adsorption phenomenon, and SG adsorption ability is very stable even with a long time of use. SG is also used as an adsorbent due to its high adsorption capacity, reliability, and low cost compared to other adsorbents [11]. Besides, the silica gel-water adsorption system is suitable for the low grade of heat sources [12].

The analysis of the thermal behavior of devices using silica gel was studied by Gurgel et al. [13,14]. The authors showed that silica gel is very sensitive to heat and mass transfer inside the adsorbent beds. Several modifications are used to improve the thermal properties of silica gels. Mixtures with various compounds, including nanomaterials, graphite, crystals, or chemical modifications involving the introduction of functional groups [15], can increase silica gels' adsorption capacity to gases. This dependence also applies to thermal and mechanical changes in other mesoporous and macroporous materials [16,17]. The literature describes the possibility of improving the thermal properties by using an SG composition and materials with high thermal conductivity. To improve the thermal properties of SG as an adsorption bed, some authors analyzed the effect of metallic additives on the adsorption bed. In the paper by Rezk et al. [18], the authors noted an increase in cooling capacity and COP of modified chillers caused by metallic additives to the silica bed. In Demir et al. [19], the authors used SG as the basis of the mixture and added helical pieces of metal made of copper, brass, and aluminum and sieved to separate into two fractions: 1.0–2.8 mm and 2.8–4.75 mm. They observed that the addition of 15 wt.% of aluminum chips significantly improved the silica gel bed's thermal diffusivity. In Kulakowska et al. [20], the authors demonstrated a positive effect of the addition of aluminum powder, copper powder, and carbon nanotubes on the thermal diffusivity of the adsorption bed.

Due to the nature of adsorption aggregates' work, it was essential to study the possibility of water vapor adsorption. Vapor adsorption by RD silica gel was investigated by Goldsworthy [21]. The test results showed the maximum sorption capacity at the tested temperature (300 K) of about 0.315 wt.%. The results of other authors also reported poor adsorption of vapor [22–24]. Water vapor adsorption studies at low pressures of 500–7000 Pa of A and RD types of silica gel showed the results at the level of 0.4 and 0.45 wt.%, respectively [25]. In the literature, there are also attempts to increase the adsorption of vapor by modifying the adsorbent, e.g., modifying the $CaCl_2$ silica gel increases the contact surface of the sorbent with water vapor, thus allowing the maximum sorption capacity to be reached at the level of 0.75 wt.%. [26].

Since the discovery of carbon nanotubes (CNT) more than two decades ago [27], they have been widely used as adsorbents for gases [28,29], heavy metals [30], organic compounds [31], and pollution prevention reagents [32,33], among others. They have also been successfully used as part of high-performance composite materials [34,35]. From a mechanical point of view, a noteworthy advantage of nanocomposites over conventional materials is the extremely high surface-to-volume ratio of the reinforcing phase. The reinforcing material can consist of particles, sheets, or fibers. Such a large surface area enhancement can have a huge impact on composite properties at the macroscale, even in the presence of relatively less enhancement at the nanoscale. The addition of CNTs improves the electrical and thermal conductivity of the material. Since CNT also exhibit hydrophobic properties, this enables their use in a wide range of industries. As well as other types of nanoparticles can give better optical properties, dielectric properties, heat resistance, or mechanical properties such as stiffness, strength, and resistance to wear and damage [20,36,37].

The work on creating or modeling the performance of efficient silica gel composites and CNTs is still relevant and applicable in many application pathways. In work [37], composites of single-walled and multi-walled carbon nanotubes were created for functionalization with silica composite materials. The use of such composite was aimed to show the way for various novel applications including effective earth element adsorption performance. The addition of a small amount of double-walled carbon nanotubes (2.06%) to silica gel-based aerogel produced significant improvements in tensile strength and elastic modulus [38]. The application of CNT in adsorption is limited by their characteristics: hydrophobicity/hydrophilicity, presence of functional groups, size of specific surface area, or surface charge. While the removal of contaminants from water by nanotubes is a successful method, the use of CNTs in the adsorption of inorganic compounds, including vapors and gases, may result in a reduction in sorption efficiency. This is due to the selectivity of CNTs and their unique properties. CNTs are often added to silica aerogels [39–41] to use as adsorbents for organic contaminants [42] or specific adsorption applications [43]. Model application studies are underway to improve the cooling performance of a solar-powered adsorption unit using a novel composite adsorbent with multilayer carbon nanotubes [44,45]. There are works on silica coatings reinforced with carbon nanotubes, which improve their strength and provide higher wear resistance [46].

Thermodynamically, the adsorption phenomenon is a spontaneous process during which the free energy of the system decreases. The adsorbed phase has fewer degrees of freedom than the gas phase, and therefore the entropy decreases during adsorption [47]. In consequence, the adsorption process is exothermic—the heat is produced. In contrast, desorption is an endothermic process characterized by the consumption of heat.

The isosteric preheating is the heating and pressurization stage when both the sorption bed condenser and bed evaporator valves are closed. The sorption bed operates as a closed system subjected to heating. The increase in bed temperature induces the vapor pressure inside the bed to increase, with the total amount of adsorbate in the adsorbed phase constant at the maximum concentration. This process transforms into the isobaric desorption when the vapor pressure reaches the condenser pressure (point B in Figure 1), and the bed temperature increases, which breaks the Van der Waals forces that bound the adsorbate molecules to the surface of the adsorbent. In consequence, the desorption of adsorbate vapor starts. The bed's heating continues to sustain the endothermic desorption with an opened valve between the bed and the condenser. The desorbed vapor flows into the condenser and condenses there. This stage ends when the adsorbate concentration reaches its minimum level, and the bed gains its maximum temperature (point C in Figure 1). In the next stage (isosteric precooling), both the sorption bed valves are closed, and the bed is cooled, which induces the pressure inside the bed to be reduced to the level of evaporator pressure (point D in Figure 1). In the last stage of the adsorption chiller work cycle, the valve between the sorption bed and the evaporator opens while the cooling continues to reject the exothermic adsorption's heat. This induces an adsorbate vapor to be bound to the adsorbent surface. The evaporator's vaporization process delivers the adsorbent vapor to the bed and gives the cooling effect during stage D-A depicted in Figure 1. The described cycle continues as the periodic change of adsorbent temperature is the driving force of the adsorptive cooling production process.

Energy and environment-related issues are the focus of scientific activities aiming to reduce primary energy consumption. An effective way to decrease electricity demand for cooling is to use environmentally benign, thermally powered adsorption cooling and desalination systems capable of utilizing industrial waste heat sources, solar, or geothermal energy utilizing environmentally friendly refrigerants. In comparison to conventional vapor-compression systems the recent interest in adsorption cooling and desalination technology results from the fact the adsorption systems: (1) are powered by renewable or waste heat sources of temperatures as low as 323 K [47], which directly leads to a reduction in CO_2 emissions and pollution [48], (2) are environmentally friendly due to the absence of

hazardous and environmentally harmful refrigerants [49], (3) allows producing cooling and desalinated water simultaneously [50], (4) have almost zero electricity consumption [51], (5) have no moving parts resulting in high reliability [52], (6) are quiet due to the absence of compressors and no-vibration [53], (7) are simple control & maintenance [53].

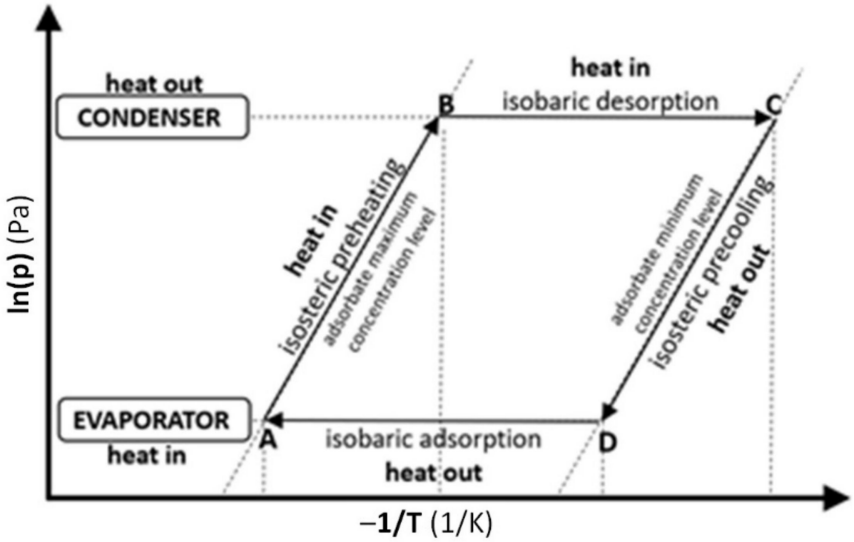

Figure 1. Stages of adsorption chiller work cycle.

However, the widespread application of adsorption chillers is limited by the shortcomings of adsorption cooling technology due to low coefficient of performance [54], bulkiness [52], intermittent cooling [55], high investment costs [55], exploitation under vacuum conditions [56].

In designing an adsorption bed, one of the many aspects to be considered is the parameters of the sorption capacity of the bed relative to water vapor. In this paper, we aim to investigate the effectiveness of a mixture of silica gels and CNTs for use in adsorption chillers. To do this, we determined the sorption capacity of vapor on silica gel enriched with CNTs, by performing isothermal sorption experiments on silica gel samples with and without CNTs. The structural properties of samples, such as specific surface area, pore volume, and pore size distribution, were analyzed using the low-pressure nitrogen adsorption method and scanning electron microscopy method. Water vapor accumulation and emission studies were carried out by gravimetric method at temperatures of 298 K, 313 K, and 333 K. The results showed that the presence of CNTs causes a decrease in the sorption capacity of silica gels in relation to water vapor. The values of sorption capacity to vapor and the effect of CNT addition are dependent on the temperature of the sorption process. As the process temperature increased, lower sorption capacity values of SG/CNT mixtures were obtained. Increasing differences in the mixture sorption capacity to water vapor were also obtained compared to pure silica gels.

2. Methods

2.1. Research Apparatus

Water vapor accumulation and emission tests using the gravimetric method were performed on a DVS VACUUM device (Surface Measurement Systems, UK, Wembley) (Figure 2). It was used to analyze sorption processes in high vacuum conditions. The analyzer works under isothermal and isobaric conditions. Before the measurement, the samples were degassed with a turbomolecular pump for 24 h at 573 K under UHV conditions. This ensured the removal of moisture from the tested materials before the proper measurements. Since the sorption rate strongly depends on temperature [12,57], measurements were carried out under isothermal conditions. Both pure materials and mixtures were tested at three temperatures: 298 K, 313 K, 333 K, in the relative humidity range of

0% < RH < 100% for the adsorption process and 100% < RH < 0% for desorption, respectively. The Brunauer Emmett Teller (BET) model was used to describe the experimental adsorption/desorption data.

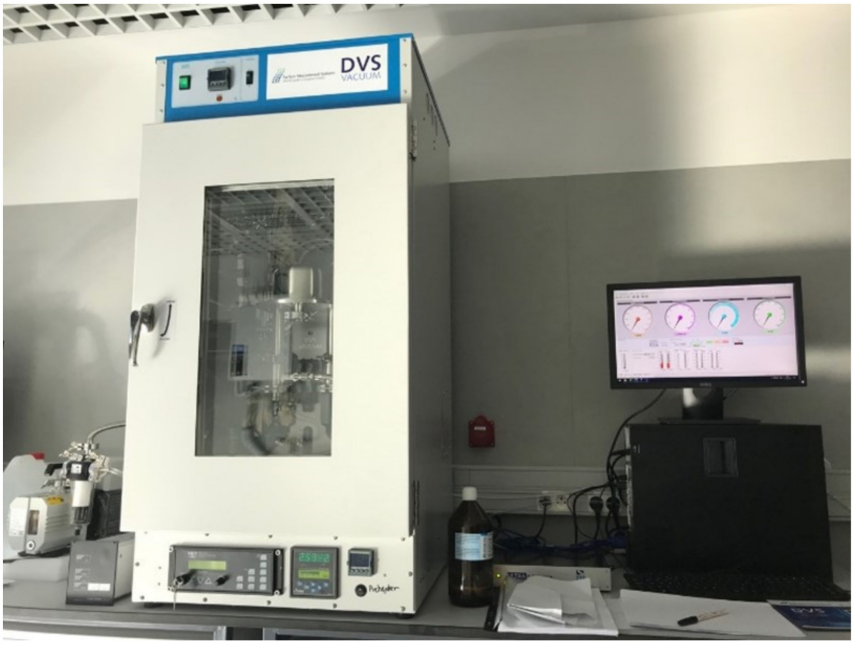

Figure 2. DVS VACUUM Dynamic Dual Vapor/Gas Gravimetric Sorption Analyzer (Surface Measurement Systems).

DVS VACUUM device (Surface Measurement Systems) is a gravimetric system designed for applications requiring vacuum conditions. Allows obtaining working pressure during the experiment of 10^{-6} mbar. The apparatus uses gravimetric analysis, which allows for precise determination of the adsorbent mass change during sorption processes. The adsorbent sample is placed in a vacuum chamber. Air is removed from the measuring space, and vacuum conditions are forced.

Under vacuum conditions, the temperature is increased, which allows for degassing the sample and removing the sorbate. After obtaining the set pressure and temperature parameters, the space surrounding the sample is filled with sorbate particles in the form of vapor of substance. The device allows continuous control of the amount of sorbate introduced and removed, which allows dynamic analysis. Water vapor can be generated in the temperature range 293–343 K in conditions up to 90% relative humidity RH.

The surface structure of the materials was determined using a low-pressure gas adsorption method (LPA) on an ASAP 2020 (Figure 3). The study consisted of measuring the volume of nitrogen (N_2) at 77 K that was adsorbed on the surface and in the pore spaces of the samples. The structure of pure SG and CNT samples was studied in the pressure range of 0–0.1 MPa. Based on the sorption equilibrium points, the specific surface area of the monolayer by the Langmuir model (SSA_L), the specific surface area of the multilayer by the BET model (SSA_{BET}), the pore volume (V_{NLDFT}), and pore distribution by the NLDFT model were determined.

Figure 3. ASAP 2020 Accelerated Surface Area and Porosity (Micromeritics).

The morphology and chemical composition of CNTs were characterized by scanning electron microscopy (SEM-EDS) on FEI Versa 3D equipped EDAX Apollo XP energy dispersive X-ray spectrometer (EDS). The elemental composition was analyzed for 50 s at accelerating voltages of 10 kV utilizing a spot analysis on the particle center. Thermal characterization of pure materials was performed by DSC-TGA using a Mettler Toledo TGA/DSC 3+ instrument. Samples (~6 mg) were combusted in an air atmosphere at 1123 K, at 10 K/min, in an air flow of 50 mL/min. Alumina crucibles of 70 µL capacity were used.

The ASAP 2020 (Micromeritics, Norcross, GA, USA) is used to analyze sorption processes by low-pressure gas adsorption (LPA). The instrument allows precise determination of the volume of adsorbate during sorption processes. The ASAP analyzer consists of two independent vacuum systems and analysis manifolds. Before measurement, samples are subjected to fully automatic degassing with controlled heating time profiles. The sample tube is connected to a buffer chamber, which ensures the isobaric conditions of the adsorption process. During the nitrogen adsorption measurement, the sample is placed in a Dewar flask filled with liquid nitrogen which ensures a temperature of 77 K and isothermal conditions. The measurement was performed in the pressure range 0–0.1 MPa.

2.2. Materials

To study water vapor accumulation and emission, a mixture of 90% by weight of two types of commercial silica gels (SG) and 10% carbon nanotubes (CNT) was used. Each type of SG had three diameters. The commercial SGs were supplied from Sigma Aldrich (Poznan, Poland) (named SG1) and Fuji K Chemical Ltd. (Greenville, SC, USA) (named SG2). CNT were produced by 3d-nano (Krakow, Poland). The CNT grew from cobalt catalyst and were synthesized by chemical catalytic deposition (CVD). The main properties of materials used in this paper are shown in Table 1. The structural (LPA), SEM-EDS, and thermogravimetric DSC-TGA analyzes were performed. The measurement results are included in Figures 4 and 5.

Table 1. Parameters of pure materials used for research.

Sample	Symbol	Granulation [μm]
Silica Gel, Sigma Aldrich	SG1a	100–160
	SG1b	200–250
	SG1c	350–400
Silica Gel, Fuji Silysia Chemical	SG2a	100–160
	SG2b	200–250
	SG2c	350–400
Carbon Nanotubes, 3d-nano	CNT	$Ø_{in}$ = 2–6 nm $Ø_{out}$ = 5–20 nm l = 10 μm

Where: $Ø_{in}$—inner diameter of the nanotube; $Ø_{out}$—outer diameter of the nanotube; l—length of the nanotube.

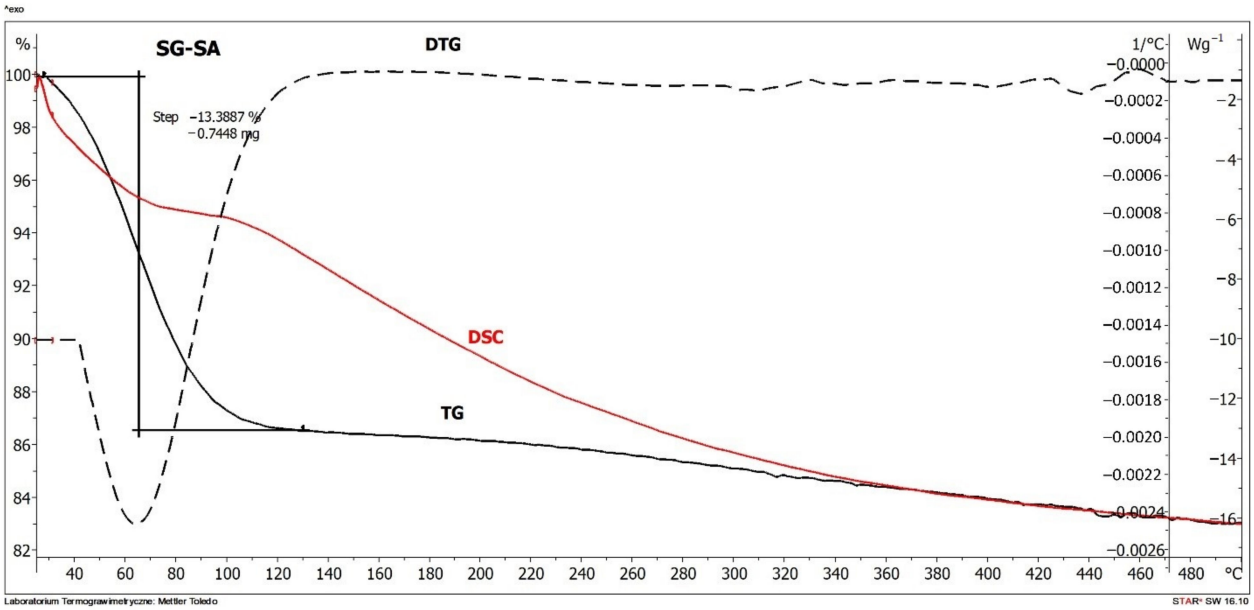

Figure 4. Thermogravimetric DSC-TG analysis of SG1a.

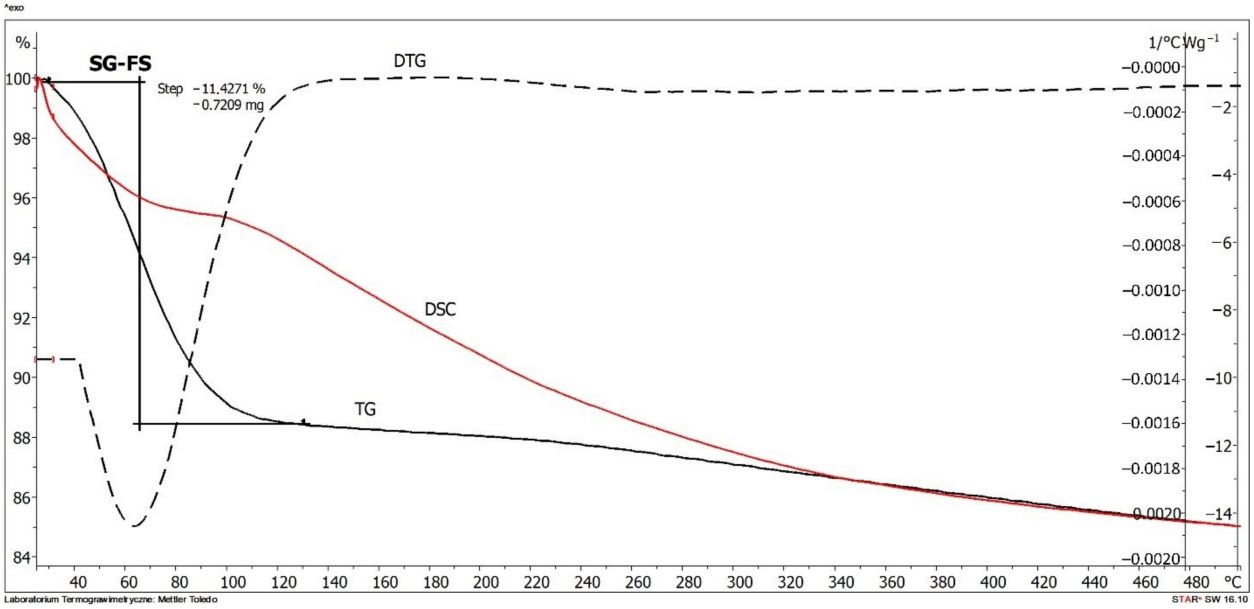

Figure 5. Thermogravimetric DSC-TG analysis of SG2a.

2.3. Structural Analysis

To select SG of different grain sizes for water vapor sorption studies, structural studies were performed first. LPA studies aimed to indicate materials for further research with the most favorable pore space parameters. The equilibrium points of N_2 adsorption on the tested silica gels had the shape of type I isotherms (Figure 6a,b). In the case of SG2, the hysteresis loop was obtained [58]. The total adsorption capacity at $p/p_0 = 1$ for SG1 samples was in the range of 8.1–11.1 mmol/g (Figure 6a), while for SG2 in the range of 10.3–12.1 mmol/g (Figure 6b). The tests showed that the grain size of the SG used affects their sorption capacity in relation to gases. The highest sorption capacity was obtained for silica gel with a granulation of 100–160 µm (SG1a and SG2a) and these samples were selected for further tests on water vapor sorption. The N_2 adsorption isotherms on CNT had the shape of type III and a small area of hysteresis loops were obtained (Figure 6c). Total sorption capacity for CNT ($p/p_0 = 1$) was 24.4 mmol/g.

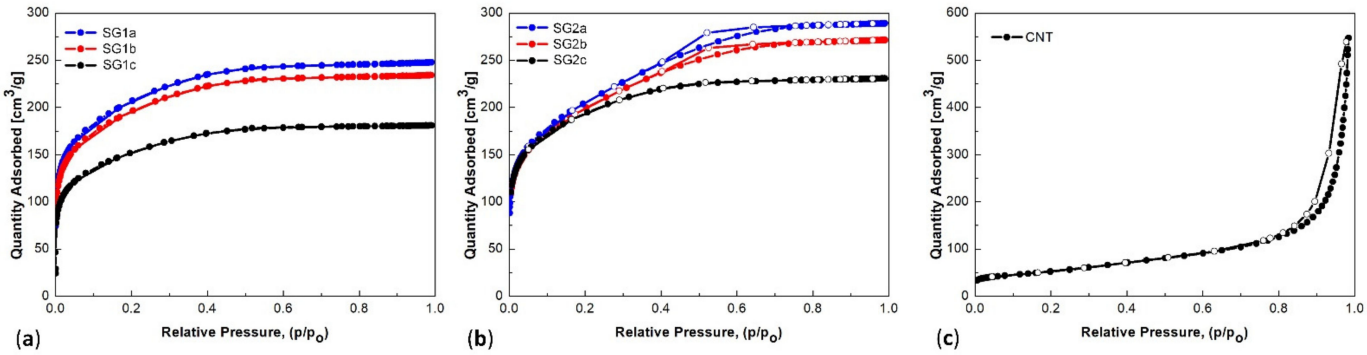

Figure 6. Nitrogen adsorption/desorption isotherms in 77 K of (**a**) SG1, (**b**) SG2, (**c**) CNT.

Based on the sorption LPA equilibrium points, structural parameters have been determined (Table 2). Due to different isothermal shapes for SGs and CNT, different models were used to describe the values of their structural parameters. The selected silica gels had a type I isotherm shape—typical for the Langmuir model [58], and the monolayer specific surface area (SSA_L) was in the range of 1127–1334 m^2/g. Total pore volume (V_t) was 0.38–0.44 cm^3/g, while volume in micropores with diameters smaller than 1 nm was 0.15 cm^3/g. In the CNT, where the shape of the isotherm was type III, which is best fitted by the BET model, the specific surface area of SSA_{BET} was 186.6 m^2/g. The total pore volume was 0.24 cm^3/g, of which the micropore volume was negligibly low.

Table 2. Structural parameters of SGs and CNT.

Parameter	Unit	SG1	SG2	CNT
BET Surface Area (SSA_{BET})	m^2/g	713.3 ± 10.9	706.8 ± 9.2	186.6 ± 0.9
Langmuir Surface Area (SSA_L)	m^2/g	1126.7 ± 8.8	1334.4 ± 31.3	429.9 ± 24.5
Volume in Pores (V)	cm^3/g	0.151 *	0.146 *	0.022 **
Total Volume in Pores (V_t)	cm^3/g	0.380 *	0.441 *	0.237 **
Area in Pores (SSA_{NLDFT})	m^2/g	0.3 *	4.4 *	0 **
Total Area in Pores ($SSA_{t\ NLDFT}$)	m^2/g	435.2 *	467.3 *	99.4 **
Standard Deviation of Fit ($NLDFT$)	cm^3/g STP	0.80	1.08	1.05
Characteristic Energy	kJ/mol	14.9	12.7	20.6

Where: results marked with *: volume in pores < 1.0 nm; total volume in pores ≤ 23.7 nm; area in pores > 23.7 nm; total area in pores ≥ 1.0 nm; results marked with **: volume in pores < 2.5 nm; total volume in pores ≤ 18.1 nm; area in pores >18.1 nm; total area in pores ≥ 2.5 nm.

The NLDFT model was used to determine the pore size distribution for the tested materials. The pore size distributions in both silica gels (Figure 7a) had similar shapes. The presence of pores with diameters of single nanometers was found (Figure 7b). The first peak shows the presence of increased pore volume with a diameter of 1–1.5 nm and had a higher value for SG1. The second volume increase was observed for pores with diameters from 2 nm to 6 nm in SG1 and from 2 nm to 10 nm in SG2. In CNT (Figure 7b), peaks of increased volume were observed in the pore range with diameters of 3–4 nm and above 5 nm.

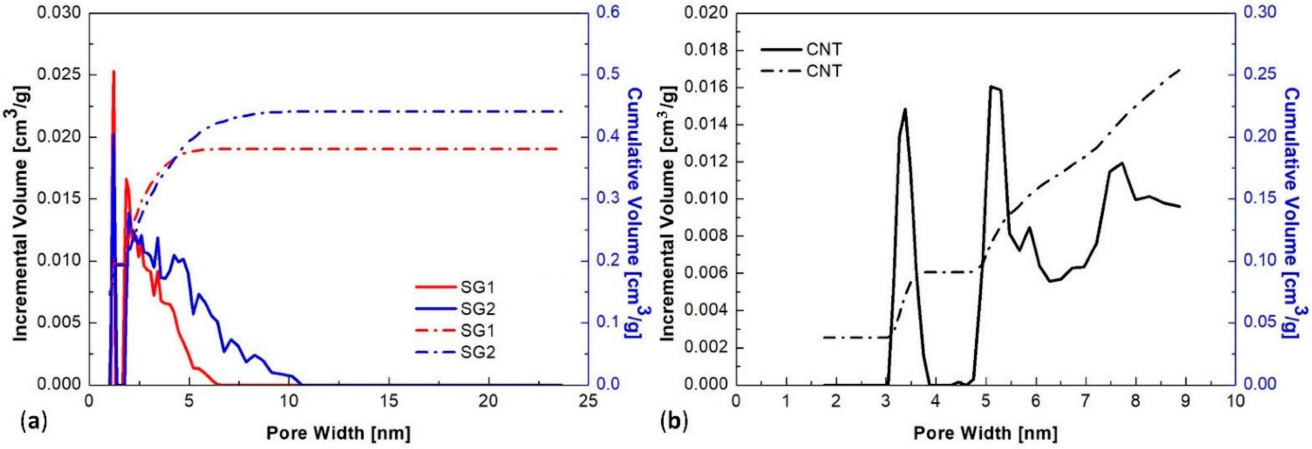

Figure 7. Pore size distribution (NLDFT method), (**a**) SG1 and SG2, (**b**) CNT.

2.4. Scanning Electron Microscopy Analysis

The selected SGs had totally different particle shapes. Silica gel SG1 with diameters of 100–160 µm (Figure 8a,b) has an uneven shape as a skew with sharp edges. Silica gel SG2 with diameters of 100–160 µm (Figure 8c,d) was characterized by a uniform spherical shape for every piece. EDS analyses confirmed the chemical purity of both materials.

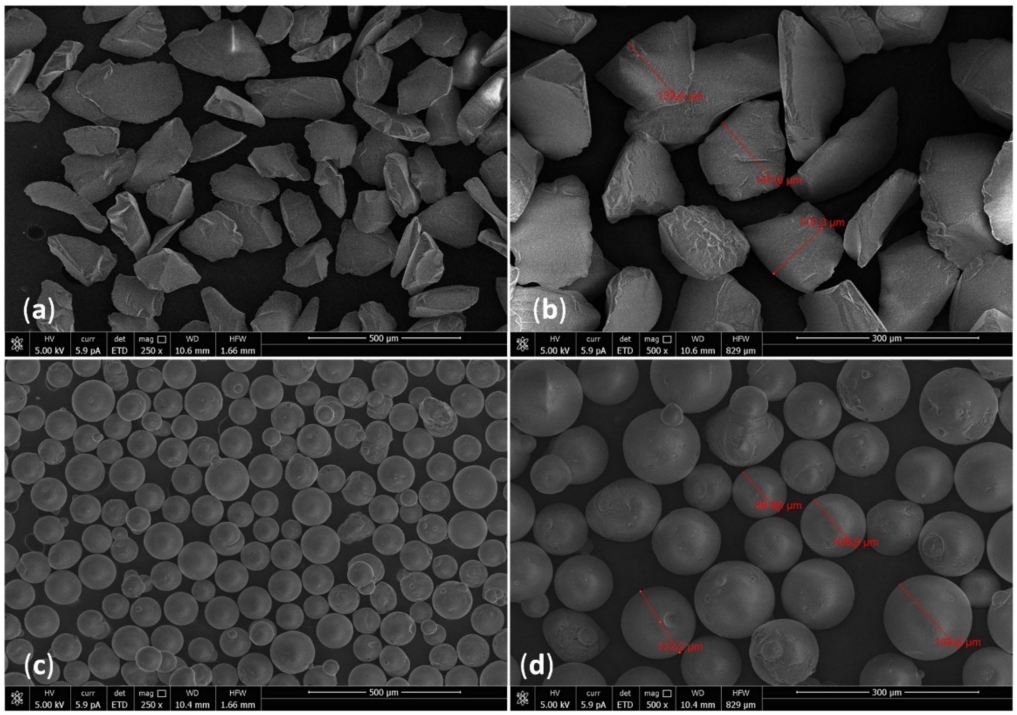

Figure 8. SEM image of the microstructure of the silica gel surface: (**a**) SG1 magn. 250×; (**b**) SG1 magn. 500×; (**c**) SG2 magn. 250×; (**d**) SG2 magn. 500×.

Figure 9a–c showed the SEM images of CNTs. CNTs form a lump consisting of nested nanotubes through a random interconnection. A porous structure is observed consisting of nanofibers of various diameters from 10 to 36 nm and a cylindrical cross-section. The EDS analysis (Figure 9d) revealed a high carbon content of 96.4 at%. The remainder is oxygen, which can be attributed to the ease of oxidation of amorphous carbon. Small amounts of magnesium, aluminum, manganese, and cobalt were also detected. The presence of trace elements may be due to surface contamination.

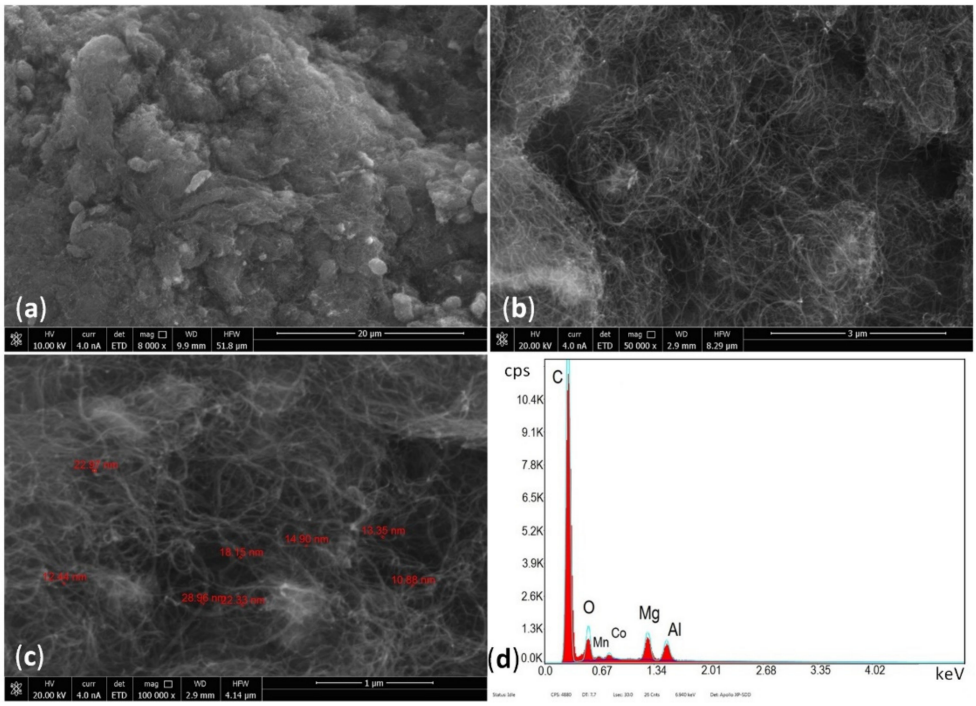

Figure 9. Multiwall carbon nanotubes CNT, (**a**) magn. 8000×; (**b**) magn. 50,000×; (**c**) magn. 100,000×; (**d**) chemical composition determined by an X-ray dispersion energy spectrometer (EDS).

3. Results

The vapor sorption isotherm curves on SGs had similar patterns at all measurement temperatures (298 K, 313 K, 333 K). They were of mixed type III and IV (IUPAC recommendation) (Figure 10) and were characteristic of weak adsorption interactions. This type of isotherms is characteristic of mesoporous materials. According to this type, sorbed water molecules become sorption sites for subsequent sorbate molecules. As reported by Zhang et al. [59], the process then takes on an island character and the so-called clusters are formed, indicating multi-particle adsorption. The samples sorption capacity to water vapor varied as a function of measurement temperature. As the temperature increased, the sorption capacity decreased, which agrees with fluid sorption research [60].

In the SG1 samples, the vapor sorption isotherms in the range of 0% < RH < 40% (298 K) and in the range of 0% < RH < 60% (313 K and 333 K) had a nearly linear course, almost proportional to the increase in moisture content, while they flattened out above these values (Figure 10). The SG1 sorption capacity to vapor at 0.1 MPa at 298 K, 313 K, and 333 K was 31.1 wt.%, 26.8 wt.%, and 29.1 wt.%, respectively. When CNTs were added, lower values of the total sorption capacity parameter were obtained in the SG1/CNT mixtures. H2-type hysteresis loops with different areas were noted in all samples. The difference between the adsorption and desorption equilibrium points at different RH points was from 3.6% to 8.9%. The distribution of hysteresis loops for each sample is included in Figure 11.

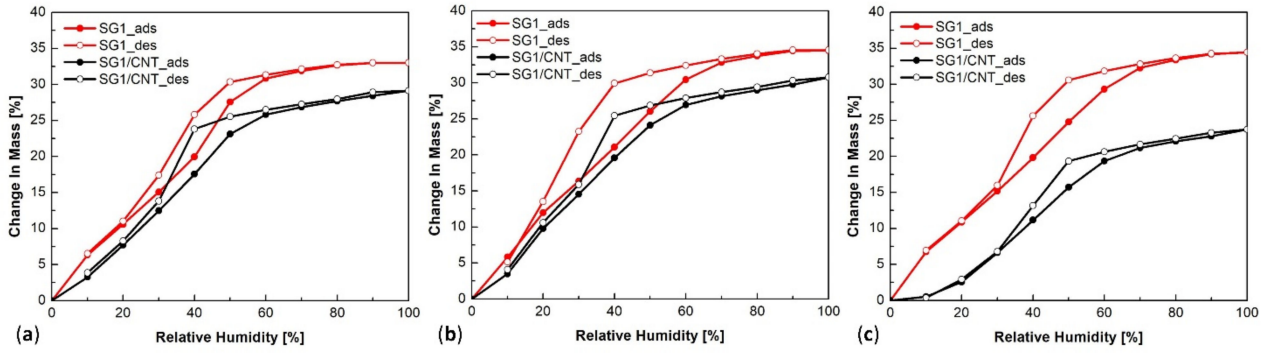

Figure 10. Adsorption-desorption isotherms of silica gel SG1 in the temperatures of: (**a**) 298 K, (**b**) 313 K, (**c**) 333 K.

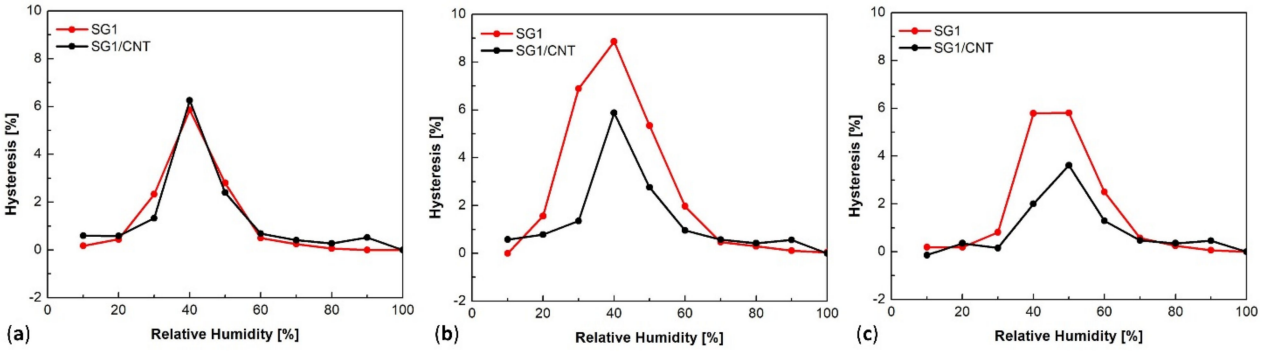

Figure 11. The difference between the isotherms of adsorption and desorption-hysteresis loop area in SG1 in temperatures: (**a**) 298 K; (**b**) 313 K; (**c**) 333K.

In the SG2 samples, the almost linear vapor adsorption isotherm was in the range of 0% to 40% relative humidity (Figure 12). From 60% < RH < 70% the isotherm curve bent and for 70% < RH < 80% the increase in adsorption was smaller and tended to plateau. A vapor total sorption capacity in the range of 23.8% wt.–35.0 wt.% was achieved. Different shapes of adsorption/desorption curves and different areas of hysteresis loops were noted in these samples, which were up to 9% (Figure 13).

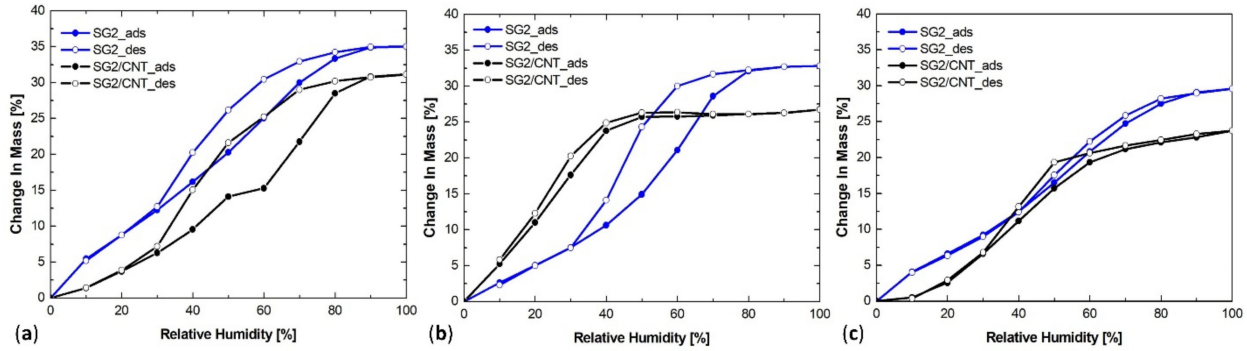

Figure 12. Adsorption-desorption isotherms of silica gel SG2 in the temperatures of: (**a**) 298 K, (**b**) 313 K, (**c**) 333 K.

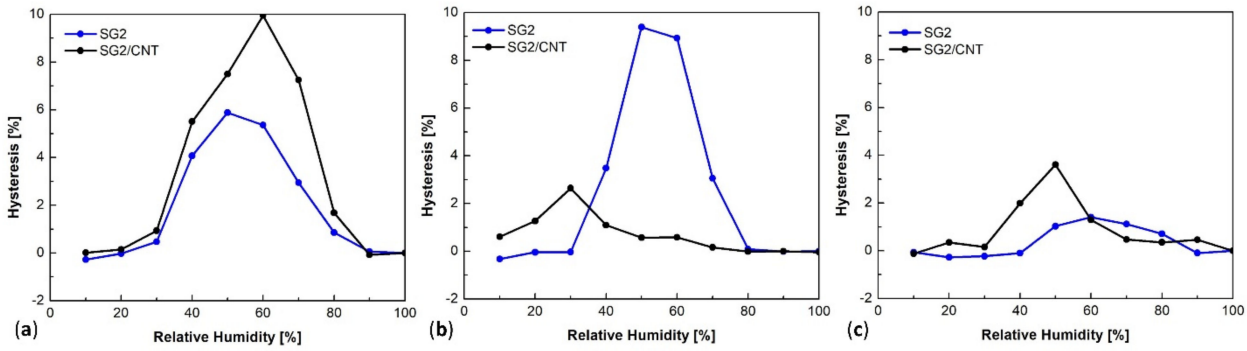

Figure 13. The difference between the isotherms of adsorption and desorption-hysteresis loop area in SG2 in temperatures: (**a**) 298 K; (**b**) 313 K; (**c**) 333K.

The use of SG/CNT mixture resulted in a decrease in the sorption capacity to vapor. As presented in Figure 14a, the ratio of change in mass in the mixture $Q_{SG1/CNT}$ to pure Q_{SG1} was less than 1. The ratio of parameter $Q_{SG1/CNT}/Q_{SG1}$ in the pressure of 0.1 MPa at 298 K and 313 K were at a very similar level of 0.88–0.89, while at 333 K it had the lowest value equal to 0.69. In the case of the SG2 silica gel, the $Q_{SG2/CNT}/Q_{SG2}$ ratio, for measurements at 298 K and 333 K, were also below 1, while at 313 K in the relative humidity range of 10% < RH < 60% it was above 1 (Figure 14b). At RH = 100% at all three temperatures, the $Q_{SG2/CNT}/Q_{SG2}$ ratio was below 1 with values in the range of 0.80–0.89, and the lowest value was obtained at 333 K.

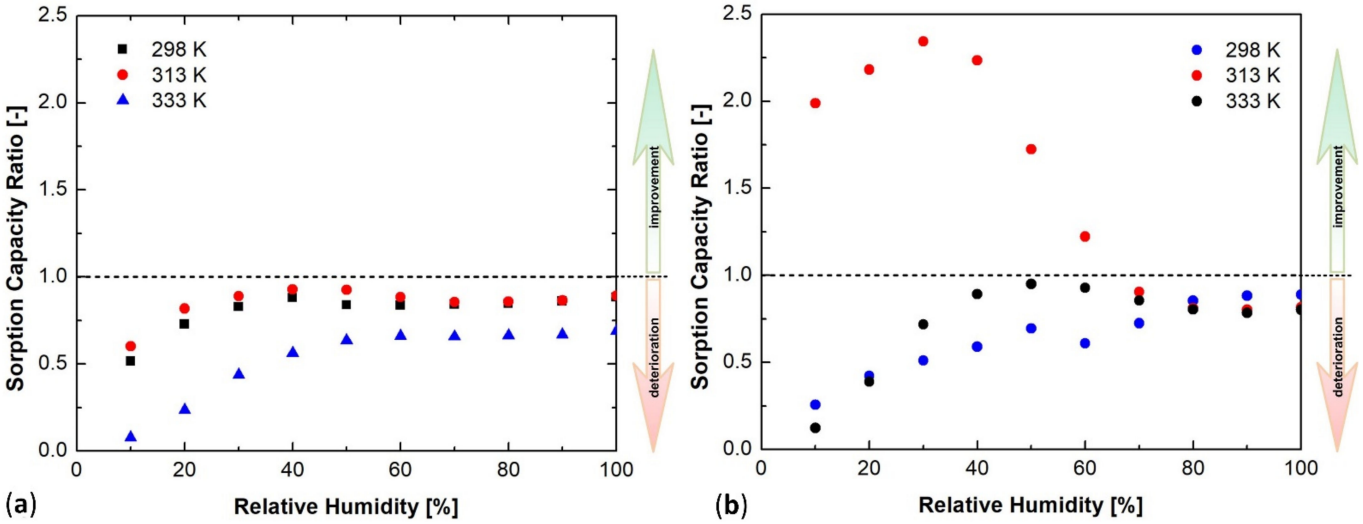

Figure 14. Ratio of sorption capacities of mixtures versus pure silica gels: (**a**) SG1 based samples; (**b**) SG2 based samples.

It was observed that the amount of adsorption increases with vapor concentration. The result was interpreted using BET isotherm. Based on the sorption equilibrium points, in the range of 0.05% < RH < 0.3%, the structural parameters were determined (Table 3). At a pressure of 0.1 MPa, the specific surface area in the SG1 sample available for vapor was in the range of 561–674 m^2/g. In the SG2, this value was at a lower level, in the range of 359–459 m^2/g. The addition of CNTs increased the vapor accessible specific surface area in the SG1/CNT mixture to 641–997 m^2/g and in SG2/CNT to 425–743 m^2/g.

Table 3. Parameters from fitting equilibrium adsorption data with adsorption isotherms.

Parameter	Unit	SG1			SG2			SG1/CNT			SG2/CNT		
Temp.	K	298	313	333	298	313	333	298	313	333	298	313	333
Q	wt.%	33	34.5	34.4	35	32.8	29.6	29.2	30.8	23.8	31.1	26.8	23.8
SSA_{BET}	m^2/g	584.8 ± 19.6	673.5 ± 77.4	560.5 ± 17.8	458.9 ± 18.5	358.8 ± 20.2	362.9 ± 38.9	840.7 ± 154	997.4 ± 198	640.8 ± 116	742.7 ± 135	517.1 ± 90.2	424.8 ± 85.5
C	-	5.17	4.11	6.12	5.95	5.44	5.06	1.46	1.39	0.92	0.66	1.45	1.9

Where: Q is equilibrium water content; SSA_{BET} is specific surface area; C is constant in BET model.

4. Discussion and Conclusions

In this paper, the sorption properties of two types of silica gels enriched with carbon nanotubes were investigated. It was proved that the granulation of silica gels affects the magnitude of their sorption capacity.

SEM-EDS investigations showed that the materials used are of high purity and that they differ significantly in particle shape. The SG2 material has a rounded shape, while SG1 has irregular shapes with sharp edges. From the vapor sorption research, the shape of the silica gel, and thus the size of the SSA_{BET} specific surface area can influence the vapor adsorption-desorption processes. Although for both silica gels similar values of the total sorption capacity were obtained at the same temperatures, the surface structure parameters were already significantly different in value.

As the study shows, the temperature and relative humidity of water vapor at an ambient pressure are the dominant factors affecting the range and rapidity of adsorption. At the same temperature, water vapor uptake increases rapidly with relative humidity. At the same humidity, although the water vapor concentration increases significantly with temperature, the water vapor uptake decreases slightly with increasing temperature, resulting in an adverse effect of temperature. Water vapor adsorption decreases rapidly with the temperature at the same water vapor concentration. The effect of temperature on the process in pure silica gels was not clear. In mixtures, worse sorption capacity parameters were obtained at higher temperatures.

The efficiency of devices using physical adsorption depends primarily on the parameters of heat and mass transport in the adsorbent bed in the form of working vapor, which must first be obtained from a specific source. An important factor determining the efficiency of the process is the thermophysical properties of the substances used in the process. The scope of the expected application and design of the device depends on the parameters of the vapor that can be obtained under given environmental conditions.

Analyses of sorption equilibrium points provide information about the sorption capacity of the adsorbent at different relative pressures or adsorbate concentrations, which is very useful for the selection of adsorbent or optimal process parameters. As can be seen from the presented results, the use of a mixture of silica gels and multi-walled nanotubes can influence the parameters of water vapor sorption in adsorption chillers. The addition of CNTs can change the sorption capacity values of the bed. The addition of 10 wt.% CNTs resulted in a decrease in the sorption capacity in mixtures. Closures of the desorption curve were obtained, which may indicate the ease of the adsorption-desorption cycle. The ratio of sorption capacities $Q_{SG1/CNT}/Q_{SG1}$ was below 1 in the whole range of tested pressures 0–0.1 MPa. For the SG2/CNT mixture, the ratio $Q_{SG2/CNT}/Q_{SG2}$ in the pressure of 0.1 MPa was also below 1. Only at 333 K and the range of 10% < RH < 60% this ratio was above 1. These results indicate the unfavorable applications of CNTs in the context of sorption. This is due to the hydrophobic properties of the tested CNTs. This is confirmed by SEM-EDS analysis, proving the purity of the nanotubes used. The presence of functional groups, both carboxyl (-COOH) and hydroxyl (-OH), is undesirable for industrial use. These functional groups block the pores of the nanotube surface and can adsorb water due to their more hydrophilic nature. The specific characteristics of CNTs related to electrical conductivity and mechanical properties, make this material nevertheless interesting for applications related to sorption as a function of temperature and pressure.

The material's other properties should also be considered. According to the literature, the addition of CNT can improve the bed-to-wall heat transfer coefficient. This results from the high conductivity of carbon nanotubes and small particle diameters, with conduction as the main mechanism of heat transfer [61].

Finally, the discussed issue should also be considered regarding the innovative idea, of the fluidized bed of sorbent application, instead of the conventional, fixed bed, commonly used nowadays in the adsorption chillers. Mixing different materials of different fluidization properties, e.g., silica gel and CNT, may facilitate fluidization and increase the bed-to-wall heat transfer coefficient [61,62].

To summarize, besides adsorption properties, other properties should also be considered when discussing the performance of adsorption cooling and desalination systems. The efficiency of devices using physical adsorption depends primarily on the heat and mass transport parameters of the adsorbent bed.

Author Contributions: Conceptualization, J.K., N.S. and A.P.; methodology, A.P., W.K., K.B. and J.L.; software, N.S. and M.K.; validation, N.S. and M.K.; formal analysis, A.P., W.K. and K.B.; investigation, A.K., A.P. and J.L.; resources, K.S.; data curation, K.S.; writing—original draft preparation, A.P. and A.K.; writing—review and editing, A.P., A.K. and M.K.; visualization, M.K.; supervision, J.K. and N.S.; project administration, A.P.; funding acquisition, J.K., A.P. and M.K. All authors have read and agreed to the published version of the manuscript.

Funding: This research was funded by National Science Center, Poland, grant number 2018/29/B/ST8/00442 and the Strata Mechanics Research Institute of the Polish Academy of Sciences as a part of statutory projects.

Institutional Review Board Statement: Not applicable.

Conflicts of Interest: The authors declare no conflict of interest.

References

1. Ammar, Y.; Joyce, S.; Norman, R.; Wang, Y.; Roskilly, A.P. Low grade thermal energy sources and uses from the process industry in the UK. *Appl. Energy* **2012**, *89*, 3–20. [CrossRef]
2. Chihara, K.; Suzuki, M. Air drying by pressure swing adsorption. *J. Chem. Eng. Jpn.* **1983**, *16*, 293–299. [CrossRef]
3. Wankat, P.C. Adsorption engineering: By Motoyuki Suzuki. *React. Polym.* **1991**, *14*, 269–270. [CrossRef]
4. Myat, A.; Thu, K.; Choon, N.K. The experimental investigation on the performance of a low temperature waste heat-driven multi-bed desiccant dehumidifier (MBDD) and minimization of entropy generation. *Appl. Therm. Eng.* **2012**, *39*, 70–77. [CrossRef]
5. Mitra, S.; Kumar, P.; Srinivasan, K.; Dutta, P. Development and performance studies of an air cooled two-stage multi-bed silica-gel + water adsorption system. *Int. J. Refrig.* **2016**, *67*, 174–189. [CrossRef]
6. Ng, K.C.; Thu, K.; Kim, Y.; Chakraborty, A.; Amy, G. Adsorption desalination: An emerging low-cost thermal desalination method. *Desalination* **2013**, *308*, 161–179. [CrossRef]
7. Thu, K.; Ng, K.C.; Saha, B.B.; Chakraborty, A.; Koyama, S. Operational strategy of adsorption desalination systems. *Int. J. Heat Mass Transf.* **2009**, *52*, 1811–1816. [CrossRef]
8. Aristov, Y.I. Challenging offers of material science for adsorption heat transformation: A review. *Appl. Therm. Eng.* **2013**, *50*, 1610–1618. [CrossRef]
9. Vodianitskaia, P.J.; Soares, J.J.; Melo, H.; Gurgel, J.M. Experimental chiller with silica gel: Adsorption kinetics analysis and performance evaluation. *Energy Convers. Manag.* **2017**, *132*, 172–179. [CrossRef]
10. Chang, W.S.; Wang, C.C.; Shieh, C.C. Experimental study of a solid adsorption cooling system using flat-tube heat exchangers as adsorption bed. *Appl. Therm. Eng.* **2007**, *27*, 2195–2199. [CrossRef]
11. Grabowska, K.; Krzywanski, J.; Nowak, W.; Wesolowska, M. Construction of an innovative adsorbent bed configuration in the adsorption chiller—Selection criteria for effective sorbent-glue pair. *Energy* **2018**, *151*, 317–323. [CrossRef]
12. Wang, D.; Zhang, J.; Tian, X.; Liu, D.; Sumathy, K. Progress in silica gel-water adsorption refrigeration technology. *Renew. Sustain. Energy Rev.* **2014**, *30*, 85–104. [CrossRef]
13. Gurgel, J.M.; Klüppel, R.P. Thermal conductivity of hydrated silica-gel. *Chem. Eng. J. Biochem. Eng. J.* **1996**, *61*, 133–138. [CrossRef]
14. Gurgel, J.M.; Filho, L.S.A.; Grenier, P.H.; Meunier, F. Thermal diffusivity and adsorption kinetics of silica-gel/water. *Adsorption* **2001**, *7*, 211–219. [CrossRef]
15. Islam, M.A.; Pal, A.; Saha, B.B. Experimental study on thermophysical and porous properties of silica gels. *Int. J. Refrig.* **2020**, *110*, 277–285. [CrossRef]
16. Pajdak, A.; Walawska, B.; Szymanek, A. The effect of structure modification of sodium compounds on the SO_2 and HCl removal efficiency from fumes in the conditions of circulating fluidised bed. *Chem. Biochem. Eng. Q.* **2017**, *31*, 261–273. [CrossRef]

17. Pajdak, A. Purification of flue gases from combustion of solid fuels with sodium sorbents. *Przem. Chem.* **2015**, *1*, 160–164.
18. Rezk, A.; Al-Dadah, R.K.; Mahmoud, S.; Elsayed, A. Effects of contact resistance and metal additives in finned-tube adsorbent beds on the performance of silica gel/water adsorption chiller. *Appl. Therm. Eng.* **2013**, *53*, 278–284. [CrossRef]
19. Demir, H.; Mobedi, M.; Ülkü, S. The use of metal piece additives to enhance heat transfer rate through an unconsolidated adsorbent bed. *Int. J. Refrig.* **2010**, *33*, 714–720. [CrossRef]
20. Kulakowska, A.; Pajdak, A.; Krzywanski, J.; Grabowska, K.; Zylka, A.; Sosnowski, M.; Wesolowska, M.; Sztekler, K.; Nowak, W. Effect of metal and carbon nanotube additives on the thermal diffusivity of a silica-gel-based adsorption bed. *Energies* **2020**, *13*, 1391. [CrossRef]
21. Goldsworthy, M.J. Measurements of water vapour sorption isotherms for RD silica gel, AQSOA-Z01, AQSOA-Z02, AQSOA-Z05 and CECA zeolite 3A. *Microporous Mesoporous Mater.* **2014**, *196*, 59–67. [CrossRef]
22. Wang, Y.; LeVan, M.D. Adsorption equilibrium of carbon dioxide and water vapor on zeolites 5a and 13X and silica gel: Pure components. *J. Chem. Eng. Data* **2009**, *54*, 2839–2844. [CrossRef]
23. Gwadera, M.; Kupiec, K.; Marszałek, A. On adsorption of water vapor on silica gel. *Czas. Tech.* **2015**, *2015*, 17–27.
24. Van Den Bulck, E. Isotherm correlation for water vapor on regular-density silica gel. *Chem. Eng. Sci.* **1990**, *45*, 1425–1429. [CrossRef]
25. Chua, H.T.; Ng, K.C.; Chakraborty, A.; Oo, N.M.; Othman, M.A. Adsorption characteristics of silica gel + water systems. *J. Chem. Eng. Data* **2002**, *47*, 1177–1181. [CrossRef]
26. Yuan, Y.; Zhang, H.; Yang, F.; Zhang, N.; Cao, X. Inorganic composite sorbents for water vapor sorption: A research progress. *Renew. Sustain. Energy Rev.* **2016**, *54*, 761–776. [CrossRef]
27. Iijima, S. Helical microtubules of graphitic carbon. *Nature* **1991**, *354*, 737–740. [CrossRef]
28. Reyhani, A.; Mortazavi, S.Z.; Mirershadi, S.; Golikand, A.N.; Moshfegh, A.Z. H_2 adsorption mechanism in Mg modified multi-walled carbon nanotubes for hydrogen storage. *Int. J. Hydrogen Energy* **2012**, *37*, 1919–1926. [CrossRef]
29. Pajdak, A.; Skoczylas, N. A comparison of the kinetics of hydrogen sorption in a metallic LaNi5 alloy and in multiwall carbon nanotubes. *Przem. Chem.* **2018**, *97*, 959–962.
30. Salam, M.A.; Makki, M.S.I.; Abdelaal, M.Y.A. Preparation and characterization of multi-walled carbon nanotubes/chitosan nanocomposite and its application for the removal of heavy metals from aqueous solution. *J. Alloys Compd.* **2011**, *509*, 2582–2587. [CrossRef]
31. Liu, F.; Fan, J.; Wang, S.; Ma, G. Adsorption of natural organic matter analogues by multi-walled carbon nanotubes: Comparison with powdered activated carbon. *Chem. Eng. J.* **2013**, *219*, 450–458. [CrossRef]
32. Ren, X.; Chen, C.; Nagatsu, M.; Wang, X. Carbon nanotubes as adsorbents in environmental pollution management: A review. *Chem. Eng. J.* **2011**, *170*, 395–410. [CrossRef]
33. Upadhyayula, V.K.K.; Deng, S.; Mitchell, M.C.; Smith, G.B. Application of carbon nanotube technology for removal of contaminants in drinking water: A review. *Sci. Total Environ.* **2009**, *408*, 1–13. [CrossRef]
34. Otero, F.; Martínez, X.; Oller, S.; Salomón, O. Study and prediction of the mechanical performance of a nanotube-reinforced composite. *Compos. Struct.* **2012**, *94*, 2920–2930. [CrossRef]
35. Hermas, A.A.; Qusti, A.H.; Salam, M.A. In situ electropolymerization of conducting polypyrrole/carbon nanotubes composites on stainless steel: Role of carbon nanotubes types. *Prog. Org. Coat.* **2012**, *75*, 404–410. [CrossRef]
36. Satishkumar, B.C.; Doorn, S.K.; Baker, G.A.; Dattelbaum, A.M. Fluorescent single walled carbon nanotube/silica composite materials. *ACS Nano* **2008**, *2*, 2283–2290. [CrossRef]
37. Ramasamy, D.L.; Puhakka, V.; Doshi, B.; Iftekhar, S.; Sillanpää, M. Fabrication of carbon nanotubes reinforced silica composites with improved rare earth elements adsorption performance. *Chem. Eng. J.* **2019**, *365*, 291–304. [CrossRef]
38. Patil, S.P. Enhanced mechanical properties of double-walled carbon nanotubes reinforced silica aerogels: An all-atom simulation study. *Scr. Mater.* **2021**, *196*, 113757. [CrossRef]
39. Bangi, U.K.H.; Kavale, M.S.; Baek, S.; Park, H.H. Synthesis of MWCNTs doped sodium silicate based aerogels by ambient pressure drying. *J. Sol-Gel Sci. Technol.* **2012**, *62*, 201–207. [CrossRef]
40. Wang, B.; Song, K.; Han, Y.; Zhang, T. Synthesis and characterization of multi-walled carbon nanotube doped silica aerogels. *J. Wuhan Univ. Technol. Mater. Sci. Ed.* **2012**, *27*, 512–515. [CrossRef]
41. Mahesh, S.; Joshi, S.C. Thermal conductivity variations with composition of gelatin-silica aerogel-sodium dodecyl sulfate with functionalized multi-walled carbon nanotube doping in their composites. *Int. J. Heat Mass Transf.* **2015**, *87*, 606–615. [CrossRef]
42. Bargozin, H.; Amirkhani, L.; Moghaddas, J.S.; Ahadian, M.M. Synthesis and application of silica aerogel-MWCNT nanocomposites for adsorption of organic pollutants. *Sci. Iran.* **2010**, *17*, 122–132.
43. Sun, T.; Zhuo, Q.; Liu, X.; Sun, Z.; Wu, Z.; Fan, H. Hydrophobic silica aerogel reinforced with carbon nanotube for oils removal. *J. Porous Mater.* **2014**, *21*, 967–973. [CrossRef]
44. Ul Qadir, N.; Said, S.A.M.; Mansour, R. Ben Modeling the performance of a two-bed solar adsorption chiller using a multi-walled carbon nanotube/MIL-100(Fe) composite adsorbent. *Renew. Energy* **2017**, *109*, 602–612. [CrossRef]
45. Sinha, S.; Milani, D.; Luu, M.T.; Abbas, A. Enhancing the performance of a solar-assisted adsorption chiller using advanced composite materials. *Comput. Chem. Eng.* **2018**, *119*, 406–424. [CrossRef]
46. López, A.J.; Rico, A.; Rodríguez, J.; Rams, J. Tough ceramic coatings: Carbon nanotube reinforced silica sol–gel. *Appl. Surf. Sci.* **2010**, *256*, 6375–6384. [CrossRef]

47. Hassan, H.Z.; Mohamad, A.A.; Alyousef, Y.; Al-Ansary, H.A. A review on the equations of state for the working pairs used in adsorption cooling systems. *Renew. Sustain. Energy Rev.* **2015**, *45*, 600–609. [CrossRef]
48. Pyrka, P. Modelowanie trójzlozowej chlodziarki adsorpcyjnej. *Zesz. Energ.* **2014**, *1*, 205–216.
49. Sur, A.; Das, R.K. Review of Technology Used to Improve Heat and Mass Transfer Characteristics of Adsorption Refrigeration System. *Int. J. Air-Cond. Refrig.* **2016**, *24*, 1630003. [CrossRef]
50. Shahzad, M.W.; Ybyraiymkul, D.; Burhan, M.; Oh, S.J.; Ng, K.C. An innovative pressure swing adsorption cycle. *AIP Conf. Proc.* **2019**, *2062*, 020057.
51. Sosnowski, M. Evaluation of Heat Transfer Performance of a Multi-Disc Sorption Bed Dedicated for Adsorption Cooling Technology. *Energies* **2019**, *12*, 4660. [CrossRef]
52. White, J. Literature Review on Adsorption Cooling Systems. *Lat. Am. Caribb. J. Eng. Educ.* **2013**, *378*, 28.
53. Sultana, T. Effect of Overall Thermal Conductance with Different Mass Allocation on a Two Stage Adsorption Chiller Employing Re-Heat Scheme. Master's Thesis, Bangladesh University of Engineering and Technology, Dhaka, Bangladesh, 2008.
54. Grabowska, K.; Sosnowski, M.; Krzywanski, J.; Sztekler, K.; Kalawa, W.; Zylka, A.; Nowak, W. The Numerical Comparison of Heat Transfer in a Coated and Fixed Bed of an Adsorption Chiller. *J. Therm. Sci.* **2018**, *27*, 421–426. [CrossRef]
55. Kurniawan, A.; Nasruddin; Rachmat, A. CFD Simulation of Silica Gel as an Adsorbent on Finned Tube Adsorbent Bed. In Proceedings of the 3rd International Tropical Renewable Energy Conference "Sustainalbe Development of Tropical Renewable Energy" (i-TREC 2018), Bali, Indonesia, 6–8 September 2018; Volume 67, p. 01014.
56. Elsheniti, M.B.; Hassab, M.A.; Attia, A.E. Examination of effects of operating and geometric parameters on the performance of a two-bed adsorption chiller. *Appl. Therm. Eng.* **2019**, *146*, 674–687. [CrossRef]
57. Shabir, F.; Sultan, M.; Miyazaki, T.; Saha, B.B.; Askalany, A.; Ali, I.; Zhou, Y.; Ahmad, R.; Shamshiri, R.R. Recent updates on the adsorption capacities of adsorbent-adsorbate pairs for heat transformation applications. *Renew. Sustain. Energy Rev.* **2020**, *119*, 109630. [CrossRef]
58. Rouquerol, J.; Avnir, D.; Fairbridge, C.W.; Everett, D.H.; Haynes, J.H.; Pernicone, N.; Ramsay, J.D.F.; Sing, K.S.W.; Unger, K.K. Recommendations for the navy. *Pure Appl. Chem.* **1994**, *66*, 1739–1758. [CrossRef]
59. Zhang, H.; Gu, W.; Li, M.J.; Li, Z.Y.; Hu, Z.J.; Tao, W.Q. Experimental study on the kinetics of water vapor sorption on the inner surface of silica nano-porous materials. *Int. J. Heat Mass Transf.* **2014**, *78*, 947–959. [CrossRef]
60. Skoczylas, N.; Pajdak, A.; Kudasik, M.; Braga, L.T.P. CH_4 and CO_2 sorption and diffusion carried out in various temperatures on hard coal samples of various degrees of coalification. *J. Nat. Gas Sci. Eng.* **2020**, *81*, 103449. [CrossRef]
61. Krzywanski, J.; Grabowska, K.; Sosnowski, M.; Zylka, A.; Kulakowska, A.; Czakiert, T.; Sztekler, K.; Wesolowska, M.; Nowak, W. Heat Transfer in Adsorption Chillers with Fluidized Beds of Silica Gel, Zeolite, and Carbon Nanotubes. *Heat Transf. Eng.* **2021**, *43*, 172–182. [CrossRef]
62. Win, K.K.; Nowak, W.; Hitoki, H.; Matsuda, M.; Hasatani, M.; Bis, Z.; Krzywanski, J.; Gajewski, W. Transport velocity of coarse particles in multi-solid fluidized bed. *J. Chem. Eng. Jpn.* **1995**, *28*, 535–540. [CrossRef]